Nanoscale

PAPER

View Article Online
View Journal | View Issue

Cite this: *Nanoscale*, 2025, **17**, 13251

Photoinduced luminescence activation of hydrophilic 'caged' carbons dots†

Aviya S. Akari, ‡ Maria R. Narciso,‡ Emmanuel O. Fagbohun, Pedro D. Ortiz, Roberto J. Botelho and Stefania Impellizzeri *

Received 10th January 2025,
Accepted 5th May 2025

DOI: 10.1039/d5nr00123d

rsc.li/nanoscale

As part of our efforts to develop nanomaterials with tunable optical properties, we devised a synthetic protocol to photoactivate the luminescence of hydrophilic carbon dots by 'caging' the nanostructures with photocleavable 2-nitrobenzyl quenchers. Photoremovable 2-nitrobenzyl groups can be attached covalently to the surface of the carbon dots *via* amide-bond formation. We show that 2-nitrobenzyls efficiently quench the emission intensity of the resulting nanoconstructs and that the luminescence can be activated upon ultraviolet illumination in solution. In addition, the carbon dots can be internalized by living cells and used as bioimaging agents.

Introduction

Photoactivatable organic dyes[1–11] and fluorescent proteins[12–18] are powerful tools for imaging with high spatiotemporal resolution in biological systems.[19–23] These weakly or non-fluorescent species can be photochemically converted to a fluorescent state when illuminated at the appropriate wavelengths, where the strategy for fluorescence activation is generally based on a photoinduced isomerization, proton transfer in the excited state, or the photoinduced cleavage of appropriate functional groups. For the latter, 2-nitrobenzyl (2NB) groups have often been used to quench the fluorescence of complimentary fluorescent dyes,[16,24–26] or even semiconductor quantum dots.[27–29] The chemical conjugation (to a dye's skeleton) or surface functionalization (of semiconductor nanoparticles) with 2NB can effectively 'cage' the fluorophore, rendering it inactive until pulsed with ultraviolet light, which frees the luminescent parent species along with a nitrosocarbonyl product.[30] Herein, we sought to determine whether 2NB groups could be used to quench the luminescence of hydrophilic carbon dots until photochemically released from the nanoparticles' surface (Fig. 1).

Over the last few years, carbon dots (CDs) have emerged as outstanding 'green' nanoprobes for fluorescence imaging and microscopy.[31–34] This is due to numerous benefits, such as the low cost, sustainability, and availability of the precursors, facile synthetic protocols and subsequent chemical modifications (thanks to the presence of COOH, OH and NH_2 groups on their surface), tunable emission and excitation, good biocompatibility and low toxicity. Moreover, CDs are intrinsically soluble in water, unlike synthetic dyes and most of their semiconductor-based counterparts. Due to these reasons, CDs are gradually replacing conventional organic dyes and inorganic quantum dots in a diversity of biomedical applications.[35–38] Thus, the identification of a mechanism to photoactivate the fluorescence of CDs can translate into the development of photoactivatable probes with improved performance. In this work, we report an easy synthetic method for the bottom-up

Department of Chemistry and Biology, Toronto Metropolitan University, 350 Victoria St, Toronto, ON, M5B 2K3, Canada. E-mail: simpellizzeri@torontomu.ca

†Electronic supplementary information (ESI) available: Materials and methods; synthesis of carbon dots (CDs **1**); conjugation of 2-nitrobenzylamine to CDs (2NB-CDs **2**); synthesis of model quencher compound 2NB-OMe (**3**); cell culture and pinocytosis of CDs **1**; cell culture and photoinduced uncaging of 2NB-CDs **2**; live-cell confocal microscopy; image and statistical analysis; TEM images and size distribution of CDs **1**; DLS profile and zeta potential of CDs **1**; XPS spectra of CDs **1**; FT-IR of CDs **1**; ^{1}H and ^{13}C NMR of CDs **1** and their precursors; determination of quantum yield of CDs **1**; emission spectra of molecular precursors; emission quenching and Stern–Volmer plot of CDs **1** with increasing amounts of **3**; voltammetry of CDs **1**; photostability of CDs **1** under UVA irradiation; emission of 2NB-CDs **2** before and after UVA irradiation in H_2O at pH 3 and 50 : 50 H_2O : DMSO; microscopy and statistical analysis of RAW 264.7 macrophages exposed to 2NB-CDs **2**. See DOI: https://doi.org/10.1039/d5nr00123d

‡A. S. Akari and M. R. Narciso made equal contributions to this work.

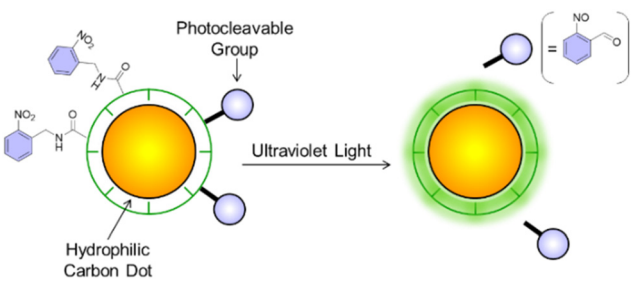

Fig. 1 Photoinduced uncaging and fluorescence activation of 2-nitrobenzyl carbon dots.

synthesis of CDs, a viable experimental protocol to couple 2-nitrobenzyl groups to our carbon nanoparticles, and the photochemical and photophysical properties of the resulting nanostructured composites before and after photoactivation.

Results and discussion

Synthesis and characterization of hydrophilic carbon dots

N-doped, COOH (surface) functionalized CDs (CDs **1**) were synthesized through an easy microwave-assisted treatment of glucosamine hydrochloride and the amino acid β-alanine in H_2O (ESI†).[39] In recent years, the prominence of N-doped CDs in the field has increased remarkably, due to their enhanced emissive properties originating from new electronic states created by the electron-rich nitrogen groups.[40–42] Indeed, electrons trapped by these newly formed surface N-states facilitate radiative recombination and, as a result, increase average fluorescence in comparison to their undoped counterparts. After lyophilization, the size and distribution of CDs **1** were characterized by transmission electron microscopy (TEM), which revealed that the carbon nanoparticles are dispersed uniformly, ranging from 2 to 7 nm (Fig. S1†). Dynamic light scattering (DLS) indicated a hydrodynamic diameter of approximately 15 nm (Fig. S2†), consistent with measuring the nanoparticles' solvation shell and the surface functional groups. The mean zeta potential of CDs **1** (Fig. S2†) was measured as −37.37 mV. The elemental composition of CDs **1** was investigated by X-ray photoelectron spectroscopy (XPS). The survey XPS spectrum of CDs **1** (Fig. S3†) revealed the presence of C, O, N and Cl, with the elemental composition being C 62.74%, O 24.95%, N 6.74% and Cl 5.58% and peaks at 286 eV (C 1s), 400 eV (N 1s), 533 eV (O 1s) and 198 eV (Cl 2p). High-resolution scans of each peak are illustrated in Fig. S4.† The surface of CDs **1** was further probed using Fourier-transform infrared spectroscopy (FT-IR, Fig. S5†), which displays the characteristic carbonyl absorption at 1714 cm^{-1} (attributed to C=O stretching mode) and a broad absorption between 2900 (sp^3 C–H stretch) and 3320 (O–H and N–H stretch) cm^{-1}, indicating successful passivation. Nuclear magnetic resonance (NMR) plays a crucial role in the characterization of carbon dots, particularly in ensuring their proper purification—a critical step, especially for syntheses involving molecular precursors. Key studies[43,44] have demonstrated the effectiveness of NMR in characterizing carbon-based nanomaterials, helping to minimize the risk of attributing properties to molecular impurities rather than the intended carbon dots, particularly when using water-soluble organic precursors, as water dialysis may not be effective in such cases. To address this, CDs **1** were purified by centrifugation instead of dialysis (which was used only for 2NB-CDs **2**, the product obtained after coupling CDs **1** with 2-nitrobenzylamine). Characterization by ^1H NMR (Fig. S6†) reveals the

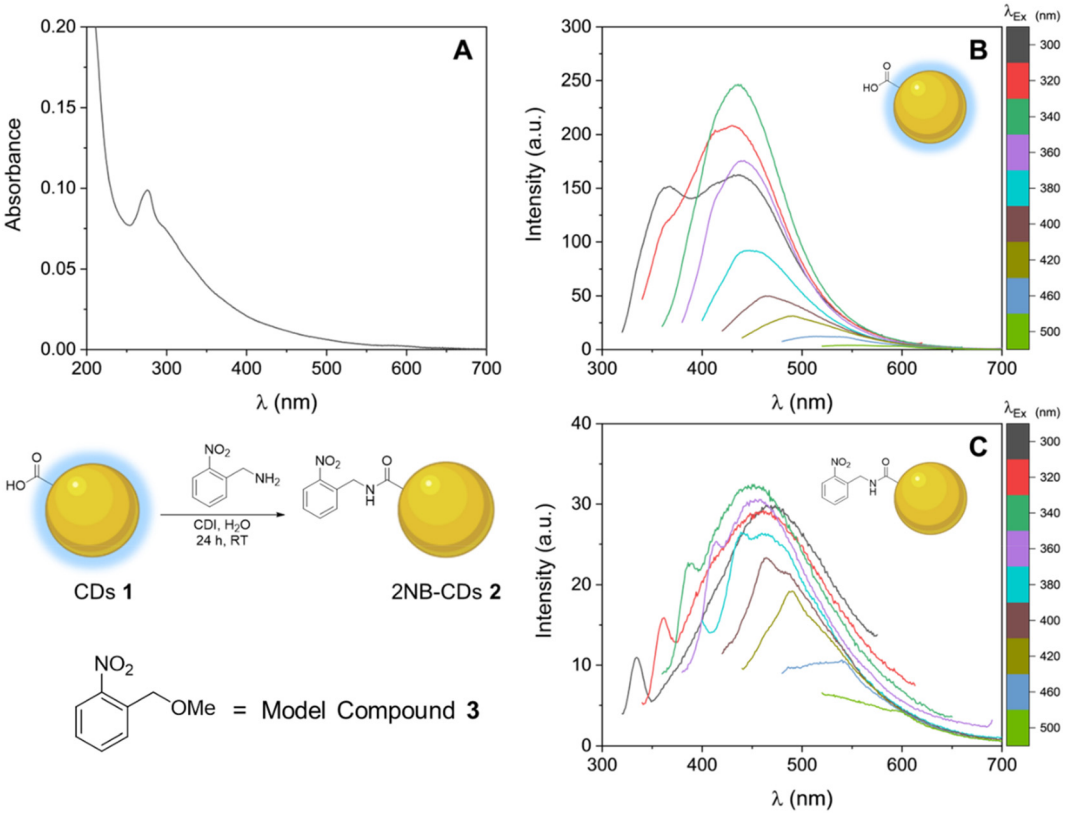

Fig. 2 Absorption (A) and emission (B) spectra (10 μg mL^{-1}, 20 °C, H_2O) of CDs **1**. Synthesis of 2-nitrobenzylamine-functionalized 2NB-CDs **2** and structure of model quencher compound **3**. (C) Emission spectra (10 μg mL^{-1}, 20 °C, H_2O) of modified 'caged' 2NB-CDs **2**.

signals expected for the β-alanine linker at 2.72 ppm (triplet) and 3.19 ppm (triplet), as well as other lower intensity absorptions which have been identified as surface-bound polyhydroxylated motifs.[39] The singlets observed at 5.08, 8.46 and 8.64 ppm can be attributed to the formation of pyrazine- and hydroxypyrazine-type architectures. The latter is also evidenced by the presence of corresponding signals between 142 and 154 ppm in the ^{13}C NMR of CDs **1** (Fig. S7†), together with the signal for sp^2 carbons of carboxylic groups peak at 175 ppm, and absorptions at 60–80 and 30–40 ppm indicative of the occurrence of sp^2 domains and sp^3 connecting structures, respectively. We compared the ^1H NMR spectrum of CDs **1** against the spectrum of a mixture of the precursors (glucosamine hydrochloride and β-alanine in the same ratio used for MW treatment) in deuterated water (Fig. S8†). We noticed remarkable differences between the spectra, the most prominent being the appearance of new peaks and patterns between 8.4 and 8.6 ppm, 5 ppm, 4 ppm and between 2.9 and 2.7 ppm (possibly indicating the formation of bonds). The disappearance of the reagent peaks can also be observed (*e.g.*, at 5.4 ppm). In addition, the peaks of the carbon dot samples are broader and decisively less defined than the precursors', which suggests that centrifugation was effective in removing molecular impurities arising from the precursors. The spectrum of CDs **1** in $CDCl_3$ (Fig. S9†) is very different from that in D_2O, indicating that the choice of solvent can significantly affect the NMR spectra. If the carbon dots are well-dispersed in a solvent that minimizes particle interactions (*e.g.*, H_2O for the highly hydrophilic CDs **1**), the resulting spectra may show sharper peaks due to reduced aggregation and better dispersion. The UV-Vis absorption of CDs **1** ranges from 200 to 550 nm (Fig. 2A). The absorption band at 275 nm can be assigned to π–π* transitions, while absorptions at higher wavelengths are attributable to n–π* transitions.[45] The emission spectrum of CDs **1** displays the typical excitation-dependent fluorescence of nitrogen-doped CDs (Fig. 2B).[40–42] The quantum yield of luminescence (Φ) of CDs **1** was calculated to be 0.08 (8%) using 4′,6-diamidino-2-phenylindole (DAPI) as a reference (see Fig. S10† and related discussion). Note that the molecular precursors used to synthesize CDs **1** are entirely not fluorescent (Fig. S11†).

Synthesis and spectroscopy of hydrophilic 'caged' carbon dots

In order to explore the influence of photocleavable 2-nitrobenzyl groups on the luminescence of our carbon nanoparticles, we treated CDs **1** with 2-nitrobenzylamine hydrochloride (Fig. 2) in the presence of 1,1-carbonyldiimidazole (CDI). The CDI-mediated reaction enables the facile placement of caging groups onto our hydrophilic CDs through the coupling between the carboxylic acid surface groups to organic molecules with pendant primary amines (ESI†). The emission spectra of the modified carbon dots (labelled 2NB-CDs **2**, Fig. 2C) reveal a negligible change in emission wavelength but a significant decrease in emission intensity (notice the low counts on the *Y*-axis and the Raman scattering signal of water). We observed an average of 86% decrease in the intensity of the blue emission of 2NB-CDs **2** excited from 300 to 360 nm in otherwise identical conditions, while quenching is less effective for higher-wavelength emission (72% at λ_{ex} = 380 nm, 55% at λ_{ex} = 400 nm, and 38% at λ_{ex} = 420 nm, respectively). Quenching is, presumably, a result of photoinduced electron transfer from the luminescent organic core to the 2-nitrobenzyl ligand. It has already been observed that the photoluminescence of carbon dots can be quenched effectively in solution by known electron acceptors such as 4-nitrotoluene, 2,4-dinitrotoluene, *etc.*[46] Indeed, the emission intensity of a dispersion of CDs **1** decreases significantly upon the addition of increasing amounts of the model compound 2-nitrobenzyl methyl ether (**3**) in methanol solution (A in Fig. S12†), in agreement with the expected photoinduced electron transfer from the nanoparticles to the quencher.

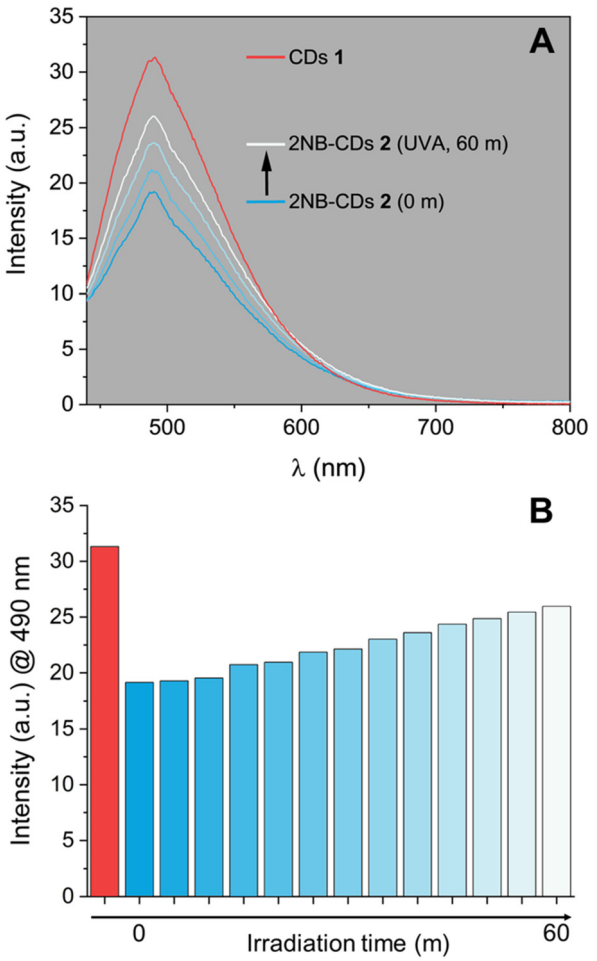

Fig. 3 (A) Emission spectra (10 μg mL^{-1}, 20 °C, H_2O, λ_{ex} = 420 nm, blue traces) of 2NB-CDs **2** before and after ultraviolet irradiation (365 nm, 0, 20, 40 and 60 min). The red trace is the emission of unfunctionalized CDs **1** recorded under identical concentration and excitation conditions. (B) Evolution of the emission intensity at 490 nm of 2NB-CDs **2** (10 μg mL^{-1}, 20 °C, H_2O, λ_{ex} = 420 nm, blue bars) recorded before and after ultraviolet illumination (0–60 m, 5 min intervals). The red bar is the emission at 490 nm of unfunctionalized CDs **1** recorded under identical concentration and excitation conditions.

Additionally, we noted a similar trend in quenching efficiency for CDs **1** + **3** to what was observed for 2NB-CDs **2** (*i.e.*, quenching is more effective at lower excitation wavelengths). The analysis of the corresponding Stern–Volmer plot indicates an association constant of *ca.* 22 M^{-1} (B in Fig. S12,† recorded at λ_{ex} = 420 nm), which is coherent with values reported for similar electron acceptors such as 4-nitrotoluene (K_{SV} = 38 M^{-1}) and 2,4-dinitrotoluene (K_{SV} = 83 M^{-1}).[47] Electrochemical measurements of CDs **1** (Fig. S13†) show their oxidation potential to be +1.43 V *vs.* Ag/AgCl. Knowing that the reduction potential of the 2-nitrobenzyl group is −1.10 V *vs.* Ag/AgCl, we can thus suggest the electron transfer process to be exergonic with a free energy change of ∼−1.27 eV (see ESI† and related discussion). Our results highlight interesting phenomenological similarities between CDs and semiconductor quantum dots: in fact, the luminescence of both species can be quenched upon surface functionalization with nitrobenzyl moieties. The possibility that the emission of carbon dots might also have a component of radiative recombination of surface-trapped electrons and holes, similar to the emission mechanisms of traditional semiconductor quantum dots (despite carbon not being a member of the semiconductor family), was suggested.[46] This interpretation is also consistent with the observed quenching of the photoluminescence of carbon dots upon surface passivation, which disrupts radiative recombinations. Quenching of the CDs' emission could also be interpreted based on the presence of emitting chromophores within the core formed during nanoparticle synthesis, which is one of the possible mechanisms of fluorescence for nitrogen-doped CDs fluorescence.[40–42] All of these considerations, and particularly our experimental determination of the oxidation potential of CDs, point toward quenching by photoinduced electron transfer from CDs **1** to 2-nitrobenzyl.

Upon 60 min of ultraviolet illumination, the emission intensity of 2NB-CDs **2** excited at λ_{ex} = 420 nm irreversibly increases (blue traces in Fig. 3) and, eventually, approaches that recorded before ligand adsorption (red trace in Fig. 3) up to 83%.[48,49] On the contrary, the control irradiation of unmodified CDs **1** under identical excitation conditions (Fig. S14†) shows a decrease in the luminescence, likely due to photobleaching. These observations suggest that the photolysis of the organic ligand removes the quencher from the surface of the carbon dots, suppresses the electron-transfer pathway and activates their luminescence.[49] The increase in luminescence observed is analogous to what was reported for photoactivatable semiconductor CdSe–ZnS quantum dots in PBS.

After 60 minutes of ultraviolet illumination at pH 3 (A in Fig. S15†), the emission intensity of 2NB-CDs **2**, excited at λ_{ex} = 420 nm, shows an irreversible increase. This trend is similar to what was observed at pH 7, although we should be cautious about making quantitative comparisons between samples recorded under different conditions. We also tested the photo-

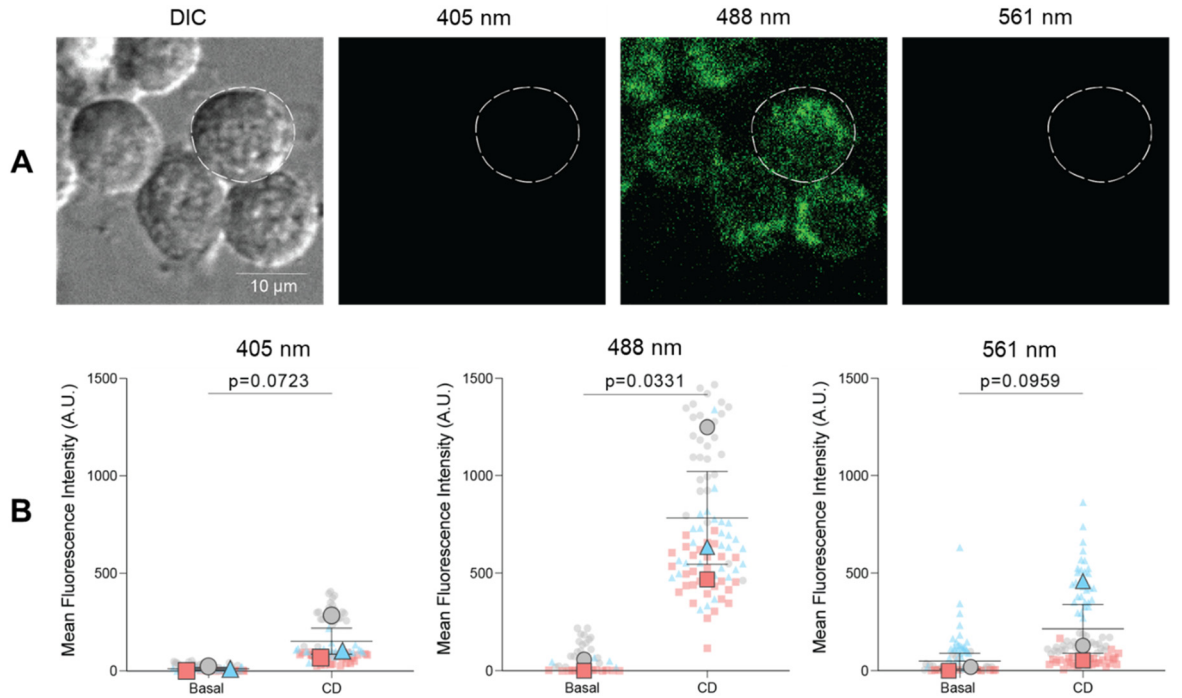

Fig. 4 (A) Spinning disc confocal microscopy of RAW 264.7 macrophages exposed to 30 mg ml^{-1} CDs **1** for 30 minutes at different excitation wavelengths. The white dashed outline indicates the position of a cell within the same field of view. (B) Mean fluorescence intensity was determined using ImageJ/FIJI. The different colours and shapes indicate replicates, n = 3 independent experiments. Outlined symbols indicate mean of replicate, with corresponding smaller symbols representing individual cell value, whereby 30–50 cells were measured per experiment and condition. Data are shown as mean fluorescence intensity per cell ± standard error of the mean after background subtraction. Data was analysed using paired, one-tailed Student's t-test. Significant comparisons used a threshold of $p < 0.05$; actual p values are shown.

chemical activation of 2NB-CDs **2** in a 50 : 50 mixture of H_2O and DMSO (B in Fig. S15†). The behaviour can generally be considered reproducible, although we noticed evidence of particle agglomeration upon the addition of the organic solvent (this was not noted at spectroscopic concentrations but in higher concentrated samples during solubility tests). Overall, however, the photochemical behaviour is considered consistent.

Fluorescence imaging of live cells

We assessed the ability of our carbon dots to undergo cellular internalization. To determine the uptake of the nanoparticles in cells, we first pulsed RAW 264.7 macrophages with 30 mg ml^{-1} of CDs **1** for 30 min, followed by a 30 min chase in a CDs-free medium. We then imaged the living cells using spinning disc confocal microscopy operating at an excitation wavelength of 405 nm, 488 nm, or 561 nm. Under these labelling and imaging conditions, we observed that cells that pinocytosed CDs **1** readily fluoresced under excitation at 488 nm compared to unlabelled cells or when excited at 405 (due to photobleaching under laser excitation) and 561 nm (Fig. 4). Moreover, the fluorescence appeared as puncta within cells, supposedly labelling lysosomes (Fig. 4A).

The photoinduced luminescence enhancement observed in aqueous environment (Fig. 3), combined with the established ability of CDs **1** to be internalized in cells, prompted us to

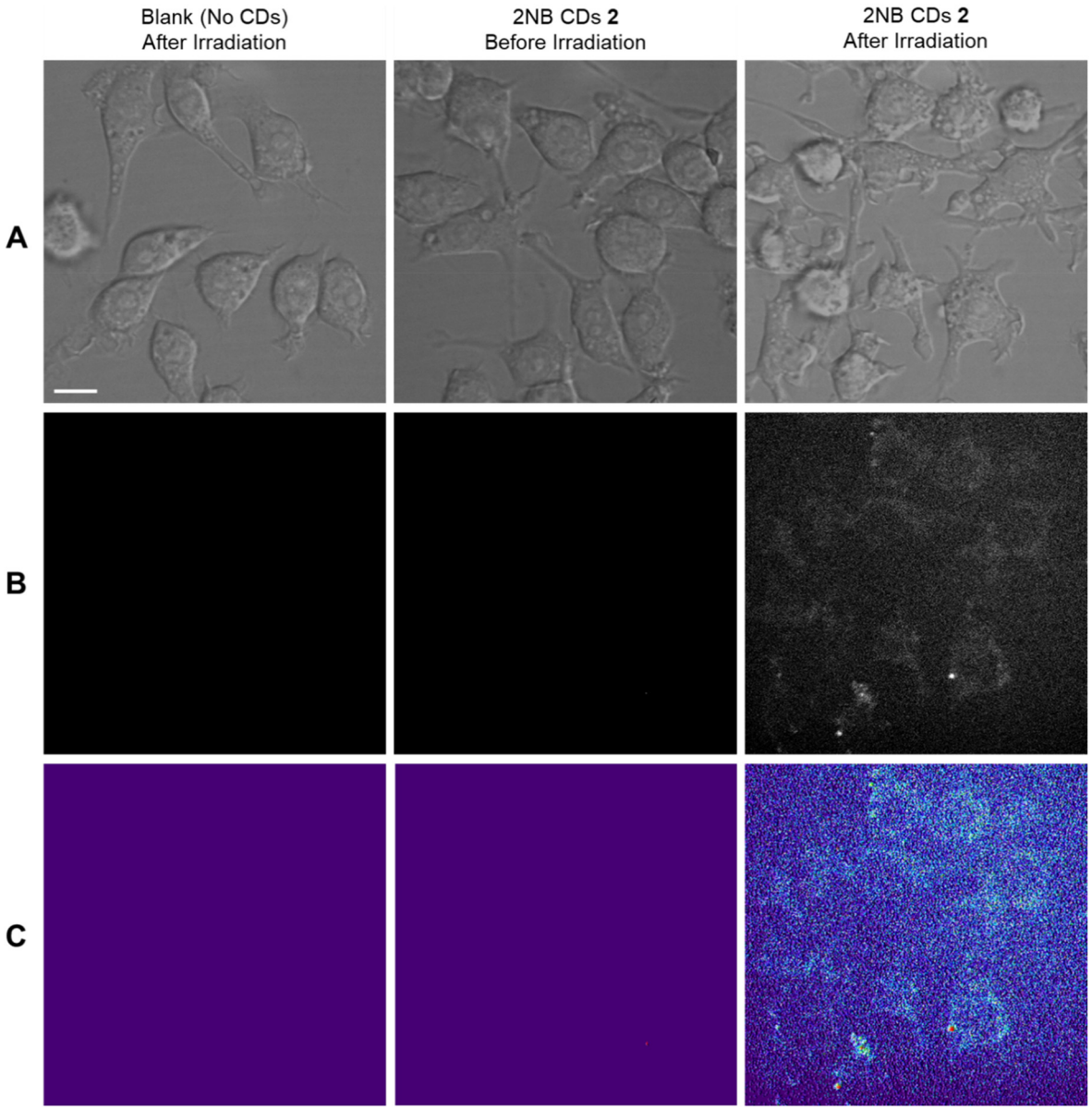

Fig. 5 Brightfield (A), luminescence (B, λ_{ex} = 488 nm) images and three-dimensional surface projections (C) of RAW 264.7 macrophages without (first column) and with (second and third column) 2NB-CDs **2** before and after ultraviolet irradiation for 30 minutes. All images were processed identically. The scale bar is 10 μm.

explore the intracellular behaviour of their caged counterparts that carry photocleavable quenchers on their surface and investigate the viability of their photochemistry. We thus attempted to label cells with 2NB-CDs **2** and image them before and after photoactivation. After ultraviolet illumination, the emission intensity of the internalized carbon dots within cells increased (particularly at λ_{ex} = 488 nm where emission is stronger, Fig. 5) but not significantly enough (Fig. S16†) before causing phototoxicity, presumably due to the long (30 minutes) exposure times. The *in vitro* pre-activation of 2NB-CDs **2**, followed by endocytosis of the uncaged nanoparticles, also did not lead to a significant level of fluorescence in cells (results not shown). However, we emphasize that the cellular internalization of carbon dots that have been photochemically uncaged *in vitro* might require different conditions than those used for CDs **1** since the photoreleased particles are expected to be structurally different on their surface.[49] Indeed, while the interaction of nanoparticles with cells is known to be significantly influenced by particle size, there is still limited understanding of the role that surface chemistry and charge have on the cellular internalization and intracellular trafficking of nanostructures.

Conclusions

We have endowed carbon dots with the ability to be switched on under optical stimulation. The hydrophilic surface of carbon dots was functionalized with photocleavable 2-nitrobenzyl groups through amide-bond formation. The 2-nitrobenzyl caging groups efficiently quench carbon dots' luminescence. Control experiments indicate that the quenching occurs through photoinduced electron transfer from the carbon dots to 2-nitrobenzyls. Upon ultraviolet illumination of the resulting nanoconstructs in water, the 2-nitrobenzyl appendages are removed from the nanoparticle surface. This process disrupts the electron transfer pathway responsible for quenching and results in the enhancement of the nanoparticle luminescence. The photolysis of 2-nitrobenzyl groups can thus be exploited to activate the luminescence of carbon dots in aqueous solutions. Moreover, the hydrophilicity of the nanoparticles facilitates their intracellular internalization, and biological imaging experiments demonstrate that our carbon dots can accumulate and emit fluorescence within living cells. Ultraviolet illumination of photocaged carbon dots internalized in cells presumably triggers the intracellular cleavage of the 2-nitrobenzyl quenchers, yielding a weak luminescent enhancement. While further modifications to the photocleavable nanoconstructs are indeed required for their effective use in a biological context, our findings highlight the potential of exploiting the photolysis of 2-nitrobenzyl groups to activate the luminescence of hydrophilic carbon dots. The inherent biocompatibility and synthetic sustainability of carbon dots make them excellent candidates for the development of new photoactivatable probes for biological imaging with improved spatial and temporal resolution.

Data availability

The authors confirm that the data supporting the findings of this study are available within the article and its ESI.†

Conflicts of interest

The authors declare no competing financial interests.

Acknowledgements

We thank the Natural Sciences and Engineering Research Council of Canada (Discovery Grant, RGPIN-2018-0416) and Toronto Metropolitan University for supporting S. Impellizzeri's research program. R. J. Botelho and M. R. Narciso's contributions to this work were funded by the Natural Sciences and Engineering Research Council of Canada (Discovery Grant, RGPIN-2020-04343), the Canada Research Chair Program (950-232333) and contributions by Toronto Metropolitan University, the Canada Foundation for Innovation and the Ontario Ministry of Economic Development, Job Creation and Trade (38151). This research has also been supported by the Toronto Metropolitan University Faculty of Science Dean's Research Fund. A. S. Akari and M. R. Narciso acknowledge the receipt of a Toronto Metropolitan Graduate Scholarship. E. Fagbohun acknowledge the receipt of an Ontario Graduate Scholarship.

References

1 H. Li and J. C. Vaughan, *Chem. Rev.*, 2018, **118**, 9412–9454.
2 F. M. Raymo, *J. Phys. Chem. Lett.*, 2012, **3**, 2379–2385.
3 Y. Zhang, Y. Zheng, Y. Meana and F. M. Raymo, *Chem. – Eur. J.*, 2021, **27**, 11257–11267.
4 D. Puliti, D. Warther, C. Orange, A. Specht and M. Goeldner, *Bioorg. Med. Chem.*, 2011, **19**, 1023–1029.
5 L. Wang, M. S. Frei, A. Salim and K. Johnsson, *J. Am. Chem. Soc.*, 2019, **141**, 2770–2781.
6 T. Ha and P. Tinnefeld, *Annu. Rev. Phys. Chem.*, 2012, **63**, 595–617.
7 L. M. Wysocki and L. D. Lavis, *Curr. Opin. Chem. Biol.*, 2011, **15**, 752–759.
8 A. N. Butkevich, M. Weber, A. R. Cereceda Delgado, L. M. Ostersehlt, E. D'Este and S. W. Hell, *J. Am. Chem. Soc.*, 2021, **143**, 18388–18393.
9 L. M. Wysocki, J. B. Grimm, A. N. Tkachuk, T. A. Brown, E. Betzig and L. D. Lavis, *Angew. Chem., Int. Ed.*, 2011, **50**, 11206–11209.
10 W. H. Li and G. Zheng, *Photochem. Photobiol. Sci.*, 2012, **11**, 460–471.
11 Y. Zhang, K.-H. Song, S. Tang, L. Ravelo, J. Cusido, C. Sun, H. F. Zhang and F. M. Raymo, *J. Am. Chem. Soc.*, 2018, **140**, 12741–12745.

12 S. Manley, J. M. Gillette and J. Lippincott-Schwartz, in *Methods Enzymol*, 2010, pp. 109–120.
13 X. X. Zhou and M. Z. Lin, *Curr. Opin. Chem. Biol.*, 2013, **17**, 682–690.
14 J. Lippincott-Schwartz and G. H. Patterson, *Trends Cell Biol.*, 2009, **19**, 555–565.
15 S. Wang, J. R. Moffitt, G. T. Dempsey, X. S. Xie and X. Zhuang, *Proc. Natl. Acad. Sci. U. S. A.*, 2014, **111**, 8452–8457.
16 G. H. Patterson, in *Current Protocols in Cell Biology*, 2008, vol. 38, ch. 21.
17 N. G. Gurskaya, V. V. Verkhusha, A. S. Shcheglov, D. B. Staroverov, T. V. Chepurnykh, A. F. Fradkov, S. Lukyanov and K. A. Lukyanov, *Nat. Biotechnol.*, 2006, **24**, 461–465.
18 K. A. Lukyanov, D. M. Chudakov, S. Lukyanov and V. V. Verkhusha, *Nat. Rev. Mol. Cell Biol.*, 2005, **6**, 885–890.
19 J. Cusido, S. Impellizzeri and F. M. Raymo, *Nanoscale*, 2011, **3**, 59–70.
20 S. T. Hess, T. P. K. Girirajan and M. D. Mason, *Biophys. J.*, 2006, **91**, 4258–4272.
21 P. Sengupta, S. B. van Engelenburg and J. Lippincott-Schwartz, *Chem. Rev.*, 2014, **114**, 3189–3202.
22 M. Fernández-Suárez and A. Y. Ting, *Nat. Rev. Mol. Cell Biol.*, 2008, **9**, 929–943.
23 Y. M. Sigal, R. Zhou and X. Zhuang, *Science*, 2018, **361**, 880–887.
24 D. Groff, F. Wang, S. Jockusch, N. J. Turro and P. G. Schultz, *Angew. Chem., Int. Ed.*, 2010, **49**, 7677–7679.
25 A. D. Erlich, N. P. Dogantzis, L. Al Nubani, L. A. Trifoi, G. K. Hodgson and S. Impellizzeri, *Phys. Chem. Chem. Phys.*, 2021, **23**, 25152–25161.
26 E. Abou Nakad, F. Bolze and A. Specht, *Org. Biomol. Chem.*, 2018, **16**, 6115–6122.
27 G. Han, T. Mokari, C. Ajo-Franklin and B. E. Cohen, *J. Am. Chem. Soc.*, 2008, **130**, 15811–15813.
28 S. Impellizzeri, B. McCaughan, J. F. Callan and F. M. Raymo, *J. Am. Chem. Soc.*, 2012, **134**, 2276–2283.
29 A. Paul, A. Jana, S. Karthik, M. Bera, Y. Zhao and N. D. P. Singh, *J. Mater. Chem. B*, 2016, **4**, 521–528.
30 P. Klán, T. Šolomek, C. G. Bochet, A. Blanc, R. Givens, M. Rubina, V. Popik, A. Kostikov and J. Wirz, *Chem. Rev.*, 2013, **113**, 119–191.
31 Q. Wang, Z. Feng, H. He, X. Hu, J. Mao, X. Chen, L. Liu, X. Wei, D. Liu, S. Bi, X. Wang, B. Ge, D. Yu and F. Huang, *Chem. Commun.*, 2021, **57**, 5554–5557.
32 S. K. Bhunia, A. Saha, A. R. Maity, S. C. Ray and N. R. Jana, *Sci. Rep.*, 2013, **3**, 1473.
33 Y. Song, S. Zhu and B. Yang, *RSC Adv.*, 2014, **4**, 27184–27200.
34 P. G. Luo, S. Sahu, S.-T. Yang, S. K. Sonkar, J. Wang, H. Wang, G. E. LeCroy, L. Cao and Y.-P. Sun, *J. Mater. Chem. B*, 2013, **1**, 2116–2127.
35 S. Anwar, H. Ding, M. Xu, X. Hu, Z. Li, J. Wang, L. Liu, L. Jiang, D. Wang, C. Dong, M. Yan, Q. Wang and H. Bi, *ACS Appl. Bio Mater.*, 2019, **2**, 2317–2338.
36 W. Su, H. Wu, H. Xu, Y. Zhang, Y. Li, X. Li and L. Fan, *Mater. Chem. Front.*, 2020, **4**, 821–836.
37 G. Ge, L. Li, D. Wang, M. Chen, Z. Zeng, W. Xiong, X. Wu and C. Guo, *J. Mater. Chem. B*, 2021, **9**, 6553–6575.
38 J. Wu, G. Chen, Y. Jia, C. Ji, Y. Wang, Y. Zhou, R. M. Leblanc and Z. Peng, *J. Mater. Chem. B*, 2022, **10**, 843–869.
39 S. A. Hill, D. Benito-Alifonso, S. A. Davis, D. J. Morgan, M. Berry and M. C. Galan, *Sci. Rep.*, 2018, **8**, 12234.
40 A. Dutta, S. T. Y. Trolles-Cavalcante, A. Cleetus, V. Marks, A. Schechter, R. D. Webster and A. Borenstein, *Nanoscale Adv.*, 2021, **3**, 716–724.
41 W. Kasprzyk, T. Świergosz, S. Bednarz, K. Walas, N. V. Bashmakova and D. Bogdał, *Nanoscale*, 2018, **10**, 13889–13894.
42 W. Wang, B. Wang, H. Embrechts, C. Damm, A. Cadranel, V. Strauss, M. Distaso, V. Hinterberger, D. M. Guldi and W. Peukert, *RSC Adv.*, 2017, **7**, 24771–24780.
43 B. Bartolomei, A. Bogo, F. Amato, G. Ragazzon and M. Prato, *Angew. Chem., Int. Ed.*, 2022, **61**, e202200038.
44 B. Bartolomei and M. Prato, *Small*, 2023, **19**, 2206714.
45 H. Ding, J.-S. Wei and H.-M. Xiong, *Nanoscale*, 2014, **6**, 13817–13823.
46 X. Wang, L. Cao, F. Lu, M. J. Meziani, H. Li, G. Qi, B. Zhou, B. A. Harruff, F. Kermarrec and Y.-P. Sun, *Chem. Commun.*, 2009, 3774–3776.
47 The carbon dots used for these reference measurements were prepared according to the procedure reported by Sun, *et al.*, *J. Am. Chem. Soc.*, 2006, **128**, 7756, and passivated with oligomeric poly(ethylene glycol) $H_2NCH_2(CH_2CH_2O)_n CH_2CH_2CH_2NH_2$. The Stern–Volmer association constant was measured at 425 nm excitation.
48 The emission intensity of 2NB-CDs **2** that were not irradiated remained unaffected after storage for weeks in the dark, indicating that the observed changes are a consequence of illumination.
49 It is important to note that the photoreleased particles are expected to be structurally different on their surface than the original (*i.e.*, before the coupling with 2-nitrobenzyl). In fact, the photochemical mechanism for the cleavage of 2-nitrobenzyl groups coupled through amide-type bonds, such as in 2NB-CDs **2**, is expected to produce carbon dots passivated with primary amides [(–C(=O)–NH_2] which might have different q.y. than [(–C(=O)–OH] passivated ones. We thus assessed the process as an 'activation', rather than 'recovery' of the emission.